Examination of Phase Transformations and Microstructural Changes on Medium Carbon Steel DIN 1.5025 under One-step Quenching and Partitioning Heat Treatment Conditions

Shima Pashangeh[1,*], Seyyed Sadegh Ghasemi Banadkouki[2]

[1]Department of Materials Engineering, Yasouj University
[2]Department of Mining and Metallurgical Engineering, Yazd University

ABSTRACT

Third-generation advanced high-strength steels serve as advanced engineering materials in various industries, including land, air, rail, and maritime transportation, with expanding applications. In the present study, a sample of low-alloy steel with medium carbon content (0.529 wt%) and high silicon content (1.670 wt%) was selected and subjected to one-step quenching and partitioning heat treatment at temperatures of 140 and 180 ºC for different partitioning times (isothermal holding for redistribution of carbon element between initial martnsite and untransformed austenite). Phase transformations and microstructural investigations were conducted using dilatometry, laser microscopy, and Electron Backscatter Diffraction (EBSD) analysis. Dilatometry results indicated that the formation of initial martensite occurs at a temperature of 275 ºC, and during a holding time of 3600 s, only carbon partitioning into retained austenite takes place at temperatures of 140 and 180 ºC, yet martensite formation occurs during the final cooling. Additionally, considering the changes in specimen width during isothermal holding, tempering of the initial martensite can be anticipated. Microstructural examinations also confirmed the formation of microphasic structures, including initial martensite, retained austenite, and final martensite.

1. Introduction

Advanced high-strength steels (AHSS) have emerged as a class of advanced engineering materials widely utilized in various industries, including automotive, railway, aviation, and maritime [1,2]. Researchers have introduced and expanded the use of these steels to address the limitations of conventional high-strength steels [2,3]. Initially, achieving both high strength and good formability in conventional steels seemed impractical. However, the demand for such steels led researchers to make significant strides in solving this challenge. Advanced High-Strength Steels (AHSS) sheets are the result of extensive efforts by researchers in this field, serving as replacements for traditional steels. These steels possess multi-phase microstructures, including martensite, bainite, and austenite phases [3,4]. Through phase transformations, they achieve enhanced hardenability, distinguishing them from conventional high-strength steels. This category of

advanced steels encompasses three different generations, with continuous advancements over time to improve their capabilities, an ongoing evolution.

The first generation of these advanced steels comprises various alloys with multi-phase microstructures based on ferrite. This generation includes diverse steels such as Dual-Phase (DP) steels, Complex-Phase (CP) steels, Martensitic (MART) steels, and Transformation-Induced Plasticity (TRIP) steels [5,6]. Currently, Dual-Phase (DP) steels are the most widely used group within the family of advanced high-strength steels. This popularity is attributed to their improved strength and formability, suitable weldability, relative ease in the manufacturing process, and their availability. Steels with deformation-induced plasticity, such as Transformation-Induced Plasticity (TRIP) steels, exhibit higher combinations of strength, flexibility, and ductility due to the transformation of retained austenite to

---

martensitic phase induced by applied strain, resulting in strain-hardening [7].

The inclination to produce steels with mechanical properties significantly superior to the first generation led to the development of advanced steels of the second generation. This generation of advanced high-strength steels predominantly features austenitic microstructures, closely related to austenitic stainless steels. The second generation includes Twinning-Induced Plasticity (TWIP) steels, Lightweight Aluminum-Induced Plasticity (IP-L) steels, and Strip-Induced Plasticity (SIP) steels [8,9]. The flexible austenitic phase of the second generation provides better formability compared to the first generation. These steels possess a significant combination of strength and ductility; however, due to the substantial increase in the production cost of alloying elements (elements required for obtaining the fine structure of the austenitic phase and stabilizing the austenitic phase, such as manganese and nickel exceeding 21% by weight for stabilizing the required austenitic phase), and challenges in the production process with practical limitations, they face restrictions [10].

Researchers in the development of each generation aim to improve mechanical properties, including strength and ductility, along with minimizing the use of alloying elements and applying simple heat treatment cycles. The third generation of advanced high-strength steels, developed to overcome the limitations of the first two generations, includes Quenching and Partitioning (Q&P) steels introduced in 2003 by Speer to obtain a unique microstructure consisting of decarburized martensite and a higher amount of carbon enriched retained austenite in leaner steels [11], as well as Nano-Bainitic steels [12] introduced by Bhadeshia. These steels exhibit desirable formability alongside high strength due to their unique microstructure, unlike many groups of advanced high-strength steels present in the first and second generations [14,15].

As mentioned, this group of advanced steels has expanded to address the deficiencies and challenges of the first two generations of these advanced materials. Different heat treatment process parametes such as quenching temperature, partitioning temperature and partitioning time as well as chemical composition of steels are the main parameters that influence the final properties of produced Q&P steels [16]. Therefore, research on this generation of advanced high-strength steels is of great importance, and undoubtedly, the research results in this field pave the way for new approaches to improve the conditions, properties, and applications of this family of engineering materials.

Considering the issues raised regarding the significance of fully investigating and understanding this group of advanced materials, and given that there is no consensus among researchers on some scientific aspects of this new group of engineering materials, the present study employs the one-step quenching and partitioning (Q&P) heat treatment method on a low-alloy steel sample with medium carbon content (DIN 1.5025). Various investigations were conducted on different aspects of phase transformations and mechanical behavior to achieve optimal conditions to attain high strength while preserving flexibility. Therefore, comprehensive examinations of microstructural studies, phase transformations, and mechanical properties were performed using various techniques on the selected initial steel sample.

2. Materials and Methods
2-1- Raw material
In the present study, a strip sample made of medium-carbon low-alloy steel with high silicon content (DIN 1.5025) was selected with the following chemical composition: 0.529C-0.721Mn-1.670Si-0.12Cr-0.023S-0.022P-Fe, based on weight percentage. Carbon and manganese elements were utilized as stabilizers for the austenitic phase [13], while silicon served as a preventer or retarder in carbide formation [18].
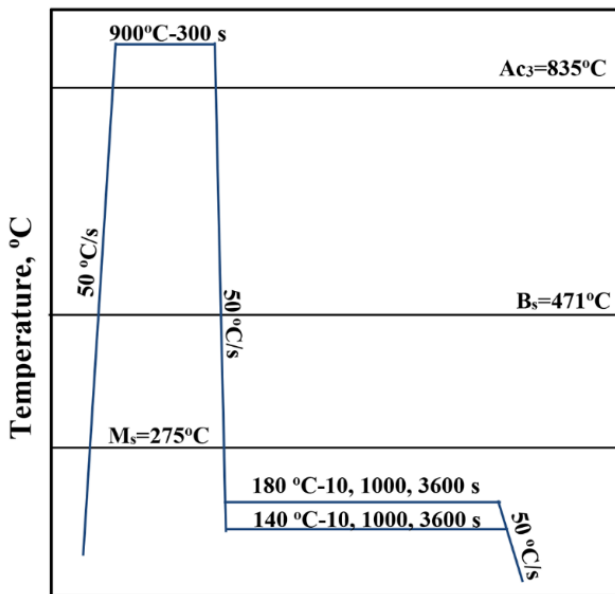
2-2- Heat treatment cycles
Before designing heat treatment cycles, critical temperatures for the selected sample were determined and calculated using dilatometry tests and theoretical relationships. The results of the tests and calculations are presented in Figure 1.

Subsequently, samples with dimensions of 3×3×1 mm were sectioned and subjected to normalizing heat treatment. For this purpose, the samples were austenitized at 900 ºC for 300 s and then cooled in the air. Following the heat treatment conditions indicated in Figure 1, the samples underwent quenching and partitioning heat treatment at temperatures of 140 and 180 ºC for durations of 10, 1000, and 3600 s. Thermal tests were

conducted using a dilatometer. Heating and cooling rates of 50 ºC/s were chosen to prevent phase transformations.

It is worth noting that the selection of temperatures at 140 and 180 ºC as partitioning temperatures, or in other words, initial quenching temperatures, will result in the formation of 80 and 90 percent volume fractions of initial martensite. These values have been calculated using the Koistinen-Marburger (K-M) equation [14] (Equation 1).

$$V_m = 1 - \exp(-\alpha_m (T_{KM} - T_Q)) \tag{1}$$

In this equation, V_m, α_m, T_{KM}, and T_Q represent the fraction of martensitic phase formed at the quenching temperature, the composition-dependent rate parameter, the theoretical temperature for the onset of martensitic transformation (281 ºC), and the quenching temperature, respectively. In this equation, α_m is taken as 0.011 (K^{-1}).

Figure 1. Schematic representation of the one-step quenching and partitioning heat treatment cycle conducted in the present study, along with the critical temperatures determined using dilatometry tests and theoretical relationships.

2-3- Microstructural investigation

In the initial step, after conducting various heat treatment cycles, samples were sectioned for microstructural examinations and then mounted using a cold mount. Subsequently, surface preparation steps were performed based on ASTM E3-01 standards. Following preparation, the final step of sample etching was carried out using a Nital solution. Preliminary examinations of the microstructure were conducted using a KEYENCE VK-X200 laser microscope with a magnification of 1500 X.

To further investigate finer details and magnify the microstructure, selected samples from different heat treatment conditions were chosen for detailed examinations using a Zeiss Ultra Plus field-emission scanning electron microscope (FE-SEM) equipped with an electron backscatter diffraction (EBSD) camera. Therefore, after surface preparation according to standard procedures and etching with a 2% Nital solution, samples were evaluated. The examinations were conducted at a magnification of 5000 X with a step size in the range of 40 to 50 nm. For this purpose, samples were electro-polished after the initial surface preparation and subjected to scrutiny.

2-4- Macro-hardness measurements

To investigate the mechanical behavior under different heat treatment conditions, macro-hardness measurements were performed using the Vickers method with an applied load of 30 Kg and a loading duration of 15 s. The reported results in this study represent the average of 5 measurements at various points on different samples subjected to various heat treatment processes.

3. Results and Discussion

3-1-Investigation of Phase Transformations Using Dilatometry Test

Figure 2 illustrates the dilatometric measurements conducted on the partitioned samples at temperatures of 140 and 180 ºC for various durations. As observed, expansion in the sample width is noticeable at different partitioning temperatures. It is worth mentioning that the oscillations seen in the initial slope of the thin-sheet samples' curves (Figures 2a and 2b) before the initiation of martensitic transformation are attributed to the device, causing changes in the slope of the curves. The curves presented in Figures 2a and 2b indicate the martensitic transformation in the temperature range of 275 ºC (region 1) before holding at temperatures of 140 and 180 ºC. Examination of the curves related to isothermal holding at different times, as shown in Figures 2c and 2d, reveals minimal expansion at the beginning of the holding time and even

contraction during prolonged isothermal holding at 180 °C. This observed expansion in the samples is related to the carbon partitioning from the initial martensitic phase, which does not transform into the retained austenite phase over time [15,16].

On the other hand, examples of sample sharp inflexions in the curves during final cooling in Figures 2a and 2b (region 3) are observed, indicating the martensitic transformation in the final stage due to the low stability of the austenitic phase even after carbon partitioning which is in agreement with previous works [21,22]. It is noteworthy that the formation of martensite is even visible after 3600 s of holding at temperatures of 140 and 180 °C, at temperatures below 100 °C

during final cooling. This suggests that after one hour of carbon partitioning from the initial martensitic phase to the remaining austenitic phase, this phase will not be stable during the final cooling to ambient temperature, and part of it will undergo martensitic transformation during the final cooling. Another reason for this phenomenon could be the occurrence of the recrystallization of the initial martensite over time, which, involves the formation of carbide particles and reduces the possibility of carbon partitioning into the austenitic phase, consequently decreasing its stability [17,18].
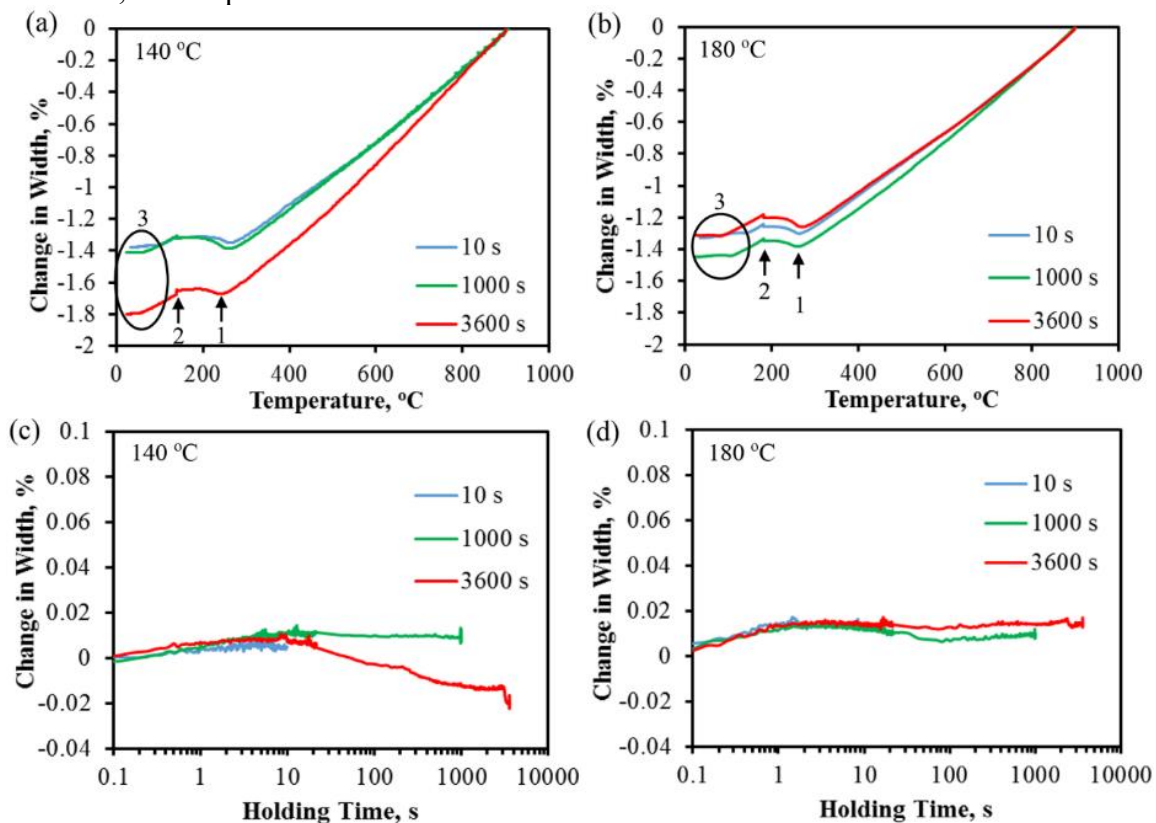
Figure 2. Variations in the width of the samples with temperature ((a) and (b)) and isothermal holding ((c) and (d)) under the conditions of the one-step quenching and partitioning heat treatment at temperatures of 140 and 180 °C were obtained using dilatometry.

The observed contraction in Figure 2d, corresponding to samples held at 180 °C after 3600 s at this temperature, may indicate the formation of carbides as a result of the recrystallization of martensite over long holding times at an isothermal condition. This phenomenon is not visible in samples held at 140 °C at various times, and even after 3600 s of holding. These results indicate that at 140 °C, due to the low temperature, a significant percentage of the martensite

tempering process, leading to carbide formation, does not occur.

3-2- Microstructural Investigation

Figure 3 illustrates the microstructural images of partitioned samples at temperatures of 140 and 180 °C for different durations: 10, 1000, and 3600 s. Figures 3a, 3b, and 3c represent the microstructures of the partitioned sample at 140 °C for durations of 10, 1000, and 3600 s, respectively. In Figure 3a, corresponding to the sample

partitioned for 10 s at this temperature, a microphasic structure is observed, including the martensite phase (light and dark gray areas) and the retained austenite phase (white areas). With an increase in partitioning time to 1000 and 3600 s, predominantly dark martensitic microstructures are observed, as shown in Figures 3b and 3c. The formation of multiphase structures, including martensite and retained austenite, under these operational conditions, has been confirmed by various researchers [19,20]. It is noteworthy that the fraction of austenite phase, initially increases and then decreases with an increase in partitioning time from 10 to 3600 s. This supports the carbon partitioning from the initial martensitic phase to the remaining austenitic phase, causing the stable fraction of this phase in the final microstructure to increase with prolonged partitioning time.
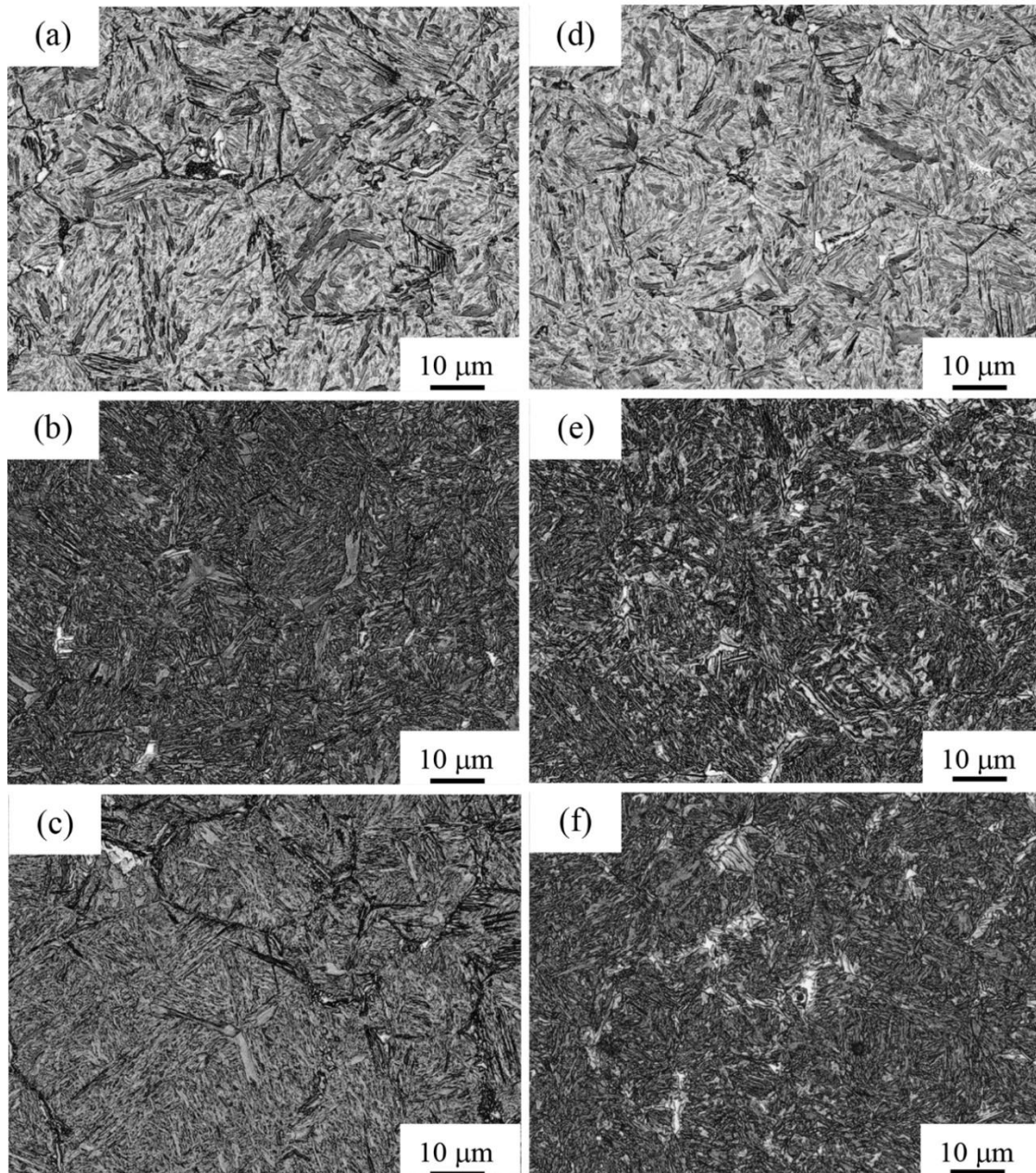
Figure 3. The laser microscope images corresponding to the partitioned samples at temperatures of 140 °C for partitioning times: (a) 10, (b) 1000, and (c) 3600 s, and at 180 °C for partitioning times: (d) 10, (e) 1000, and (f) 3600 s.

With an increase in the partitioning temperature to 180 °C, which is still below the martensite formation initiation temperature in this steel sample, the formation of multiphase microstructures similar to the partitioned samples at 140 °C is observed in Figures 3d, 3e, and 3f. Due to the fine grain structure and limitations in the magnification of laser microscopes (1500X

magnification), it is not possible to examine the formation of bainite, which would appear as very thin blades, in these microstructures. The comparison of images related to the samples partitioned at 180 °C also confirms that with an increase in the partitioning time from 10 s to 3600 s, the initial increase in the fraction of remaining austenite and its subsequent decrease with

extended partitioning time to 3600 s are observable (Figure 3f). It is noteworthy that in these images, the examination of carbide phase formation due to the annealing of the initial martensitic phase does not exist.

martensitic phase under these heat treatment conditions.
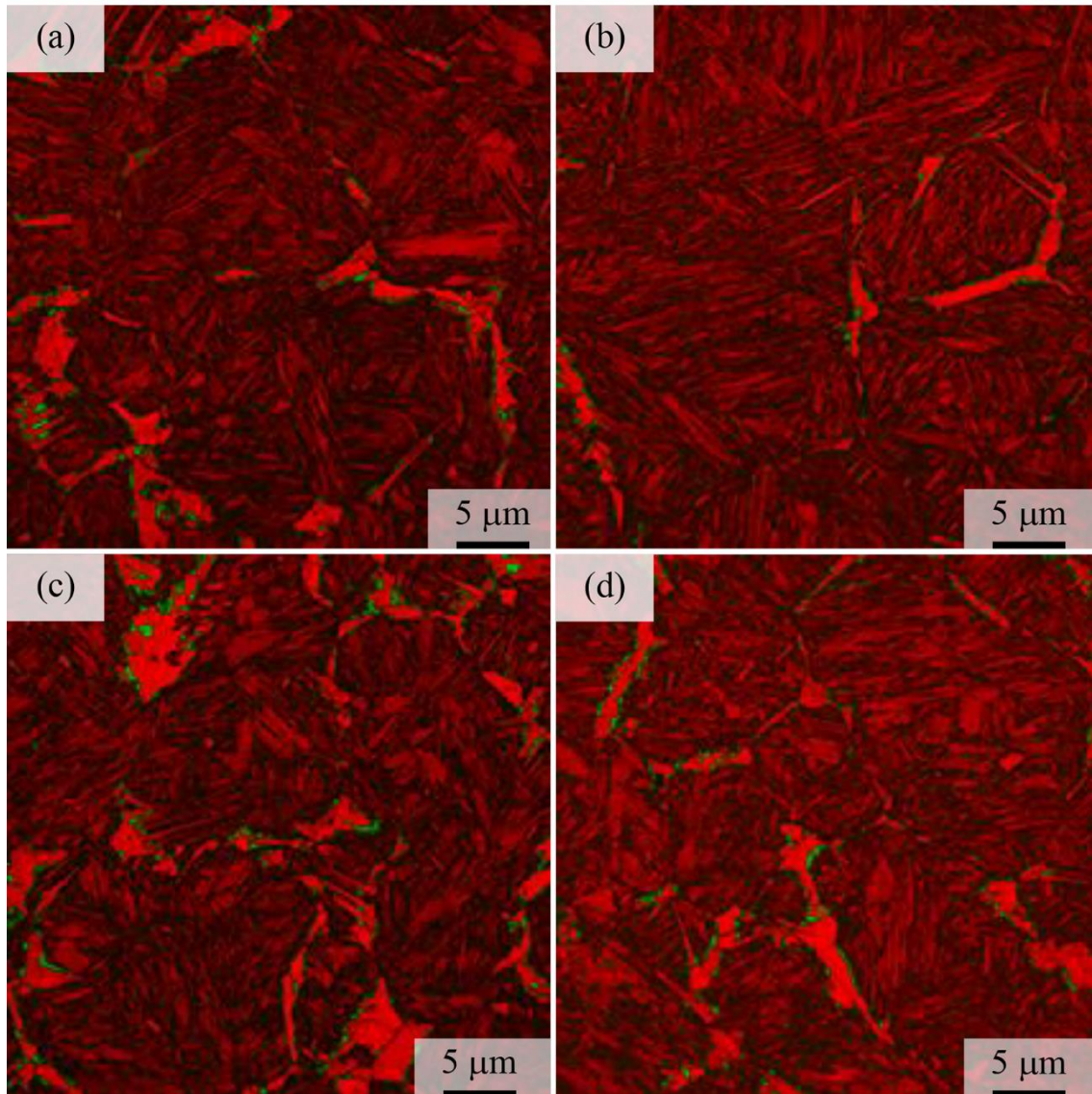
Figure 4. The EBSD images corresponding to the partitioned samples at temperatures of 140 °C for partitioning times of (a) 10 s and (b) 3600 s, as well as at 180 °C for partitioning times of (c) 10 s and (d) 3600 s.

Considering the limitations of the laser microscope in examining phases in the microstructures resulting from quenching and partitioning heat treatment, further investigation at higher samples partitioned at 140 °C for 10 and 3600 s, respectively, while Figures 4c and 4d correspond to samples partitioned for 10 and 3600 s at 180 °C. In these images, green areas represent the retained austenitic phase, while red areas indicate the martensitic phase, and if present, bainitic phase.

magnification was performed using Electron Backscatter Diffraction (EBSD) microscopy on selected samples from two partitioning temperatures. Figures 4a and 4b correspond to As observed in the images (Figure 4), the retained austenitic phase exhibits two morphologies: inter-lath in martensitic regions and blocky shapes in the initial austenitic boundary regions. Similar results have been reported by other researchers [20,21]. These two different morphology of retained

austenite phase have a different stability during TRIP effect. While blocky shape retained austenite is less stable and transform during TRIP effect, the inter-lath retained austenite is more stable [29]. The stability of retained austenite has a direct relationship with partitioning of carbon element from initial martensite to untransfomed austenite. In the inter-lath retained austenite the diffusion distance is lower and so higher value of cabon partitioning happens which directly help the austenite phase to be more stable.

On the other hand, comparing Figures 4a and 4c, which correspond to partitioning for 10 s, and Figures 4b and 4d, corresponding to partitioning for 3600 s at temperatures of 140 and 180 °C, respectively, confirms that with an increase in partitioning time, the fraction of retained austenitic phase decreases. The values for the retained austenitic phase after partitioning for 10 and 3600 s at 140 °C are 7.5% and 6%, respectively. Considering that approximately 90% of the martensitic phase is formed during the initial quenching at 140 °C, as obtained from the K-M equation, and the stability of this portion of the remaining austenitic phase does not transform in these heat treatment conditions, the final formation of the martensitic phase in the last stage of cooling, as indicated by dilatometry results, is confirmed in these images.

Additionally, according to the EBSD results the determined amount of the retained austenitic phase under partitioning conditions at 180 °C for times of 10 and 3600 s is 8.7 and 7.2 %, respectively, indicating a decrease in the percentage of retained austenitic phase due to increased martensitic tempering and less stability of the untransformed initial austenitic phase (which, as mentioned in the experimental method, had a 20% austenite fraction in the first cooling stage) which occurs in the final cooling stage. This finding confirms the formation of the martensitic phase during the final cooling, even after 3600 s of partitioning at 180 °C. These results are also consistent with dilatometric studies conducted under these heat treatment conditions

(partitioning at 180 °C), as shown in Figures 3b and 3d.

3-3- Macro-hardness measurements

The results of macro-hardness measurements for various heat treatment conditions, including quenching and partitioning at temperatures of 140 and 180 °C, are presented in Table 1. As indicated by the data in Table 1, the hardness values under partitioning conditions at 140 °C are higher than those at 180 °C. This observation is consistent with microstructural analyses and dilatometry tests, and it is attributed to the higher fraction of hard Furthermore, by examining the data in Table 1, it can be observed that the hardness values initially decrease and then increase with an increase in partitioning time up to 1000 s at 140 °C. This behavior may be attributed to the initially increased stability of the retained austenitic phase with the extended partitioning time. However, with further partitioning time, up to 3600 s, a slight increase in hardness is observed, potentially due to the reduced stability of the retained austenitic phase.

Table 1. The macro-hardness results for quenching and partitioning heat treatment conditions at temperatures of 140 and 180 °C for various partitioning times from 10 to 3600 s.

Partitioning Temperature (°C)	Partitioning Time (s)	Macro-hardness (HV$_{30Kg}$)
140	10	750
140	1000	720
140	3600	744
180	10	764
180	1000	660
180	3600	646

In contrast, under partitioning conditions at 180 °C, the hardness of the samples continuously decreases with increasing partitioning time from 10 to 3600 s, showing a direct correlation with the occurrence of the martensitic phase reversion. The results of macro-hardness measurements align well with the findings from dilatometry tests and microstructural investigations conducted in this study.

4. Conclusions

In the present study, a one-step quenching and partitioning heat treatment (Q&P) was performed on a medium carbon and high silicon low-alloy steel sample (DIN 1.5025) to investigate phase

transformations and mechanical behavior. Subsequently, the heat-treated specimens were evaluated using dilatometry tests, microstructural examinations, and macro-hardness measurements

under various conditions. The results of the conducted investigations are as follows:

1. By conducting a one-step quenching and partitioning heat treatment on DIN 1.5025 steel, the formation of multiphase microstructures, including initial martensite, retained austenite, and final martensite, was achieved.

2. The content of retained austenite in both heat treatment conditions (partitioning at 140 and 180 ºC) increased with an increase in partitioning time from 10 to 1000 s. However, with a further increase in partitioning time to 3600 s, the fraction of retained austenite decreased in the final microstructure.

3. Changes in the macro-hardness of the specimens were consistent with microstructural variations. At a partitioning temperature of 140 ºC, macro-hardness decreased with an increase in partitioning time up to 1000 s and increased with longer partitioning times up to 3600 s, corresponding to the reduced stability of retained austenite in the microstructure.

4. Macro-hardness variations under partitioning conditions at 180 ºC exhibited a descending trend with an increase in partitioning time within the range of 10 to 3600 s, attributed to the tempering of the initial martensite phase.

References

[1]   P.J. Gibbs, B.C. De Cooman, D.W. Brown, B. Clausen, J.G. Schroth, M.J. Merwin, D.K. Matlock, Materials Science & Engineering A Strain partitioning in ultra- fi ne grained medium-manganese transformation induced plasticity steel, Mater. Sci. Eng. A 609 (2014) 323–333. https://doi.org/10.1016/j.msea.2014.03.120.

[2]   D. Bhattacharya, An overview of advanced high strength steels (AHSS), in: Adv. High Strength Steel Work. Arlingt., 2006.

[3]   S. Pashangeh, M. Somani, S.S. Ghasemi Banadkouki, Structure-Property Correlations of a Medium C Steel Following Quenching and Isothermal Holding above and below the M_s Temperature, ISIJ Int. 61 (2021) 442–451. https://doi.org/10.2355/isijinternational.ISIJINT-2020-355.

[4]   S. Pashangeh, M. Somani, S.S. Ghasemi Banadkouki, Structure-property correlations of a medium C steel following quenching and isothermal holding above and below the Mstemperature, ISIJ Int. 61 (2021) 442–451. https://doi.org/10.2355/isijinternational.ISIJINT-2020-355.

[5]   J. Zhao, B. Lv, F. Zhang, Z. Yang, L. Qian, C. Chen, X. Long, Effects of austempering temperature on bainitic microstructure and mechanical properties of a high-C high-Si steel, Mater. Sci. Eng. A 742 (2019) 179–189. https://doi.org/10.1016/j.msea.2018.11.004.

[6]   D.K. Matlock, J.G. Speer, Third generation of AHSS: microstructure design concepts, Microstruct. Texture Steels (2009) 185–205.

[7]   R. Heimbuch, An overview of the auto/steel partnership and research needs, in: Adv. High-Strength Steels Fundam. Res. Issues Work. Arlington, Virginia, 2006.

[8]   A. Ramazani, K. Mukherjee, A. Abdurakhmanov, U. Prahl, M. Schleser, U. Reisgen, W. Bleck, Micro-macro-characterisation and modelling of mechanical properties of gas metal arc welded(GMAW)DP600 steel, Mater. Sci. Eng. A 589 (2014) 1–14. https://doi.org/10.1016/j.msea.2013.09.056.

[9]   N. Fonstein, Advanced high strength sheet steels: physical metallurgy, design, processing, and properties, Springer, 2015.

[10] S. Yan, X. Liu, W.J. Liu, T. Liang, B. Zhang, L. Liu, Y. Zhao, Comparative study on microstructure and mechanical properties of a C-Mn-Si steel treated by quenching and partitioning (Q&P) processes after a full and intercritical austenitization, Mater. Sci. Eng. A 684 (2017) 261–269. https://doi.org/10.1016/j.msea.2016.12.026.

[11] P. Huyghe, L. Malet, M. Caruso, C. Georges, S. Godet, Materials Science & Engineering A On the relationship between the multiphase microstructure and the mechanical properties of a 0 . 2C quenched and partitioned steel, Mater. Sci. Eng. A 701 (2017) 254–263. https://doi.org/10.1016/j.msea.2017.06.058.

[12] J. Speer, D.K. Matlock, B.C. De Cooman, J.G. Schroth, Carbon partitioning into austenite after martensite transformation, Acta Mater. 51 (2003) 2611–2622. https://doi.org/10.1016/S1359-6454(03)00059-4.

[13] H. Bhadeshia, Nanostructured bainite, in: Proc. R. Soc. London A Math. Phys. Eng. Sci., The Royal

Society, 2010: pp. 3–18.

[14] S. Kumar, S.B. Singh, Quenching and Partitioning (Q&P) Steel: Alloy Design, Phase Transformation and Evolution of Microstructure, Metall. Mater. Trans. A 54 (2023) 3134–3156. https://doi.org/10.1007/s11661-023-07085-x.

[15] S. Barella, M. Belfi, A. Gruttadauria, C. Liu, Y. Peng, Metallurgical and Mechanical Investigation on Single-Step Quenching and Partitioning Thermal Treatments on Commercial Low Alloyed 30MnV6 Steel, Metall. Mater. Trans. A 55 (2024) 513–522. https://doi.org/10.1007/s11661-023-07262-y.

[16] S. Kumar, S.B. Singh, Microstructure-property relationship in the quenching and partitioning (Q&P) steel, Mater. Charact. 196 (2023) 112561. https://doi.org/https://doi.org/10.1016/j.matchar.2022.112561.

[17] B. Mašek, H. Jirková, D. Hauserova, L. Kučerová, D. Klauberová, The Effect of Mn and Si on the Properties of Advanced High Strength Steels Processed by Quenching and Partitioning, in: PRICM7, Trans Tech Publications Ltd, 2010: pp. 94–97. https://doi.org/10.4028/www.scientific.net/MSF.654-656.94.

[18] C.J. Yu, C.-H. Seo, Y.-R. Im, D.-W. Suh, Influence of Silicon Contents on the Microstructure and Tensile Properties of Quenching and Partitioning (Q&P) Processed Low Carbon Steel, ISIJ Int. 64 (2024) 412–420. https://doi.org/10.2355/isijinternational.ISIJINT-2023-113.

[19] S.M.C.V.A.N. Bohemen, J. Sietsma, Martensite Formation in Partially and Fully Austenitic Plain Carbon Steels, 40 (2009) 1059–1068. https://doi.org/10.1007/s11661-009-9796-2.

[20] M.C. Somani, D.A. Porter, L.P. Karjalainen, P.P. Suikkanen, R.D.K. Misra, Innovation and Processing of Novel Tough Ductile Ultra-High Strength Steels Through TMR-DQP Processing Route, in: Mater. Sci. Forum, Trans Tech Publ, 2014: pp. 1009–1014.

[21] S. Pashangeh, M.C. Somani, S.S. Ghasemi Banadkouki, H.R. Karimi Zarchi, P. Kaikkonen, D.A. Porter, On the decomposition of austenite in a high-silicon medium-carbon steel during quenching and isothermal holding above and below the Ms temperature, Mater. Charact. 162 (2020) 110224. https://doi.org/10.1016/j.matchar.2020.110224.

[22] M.C. Somani, D.A. Porter, L.P. Karjalainen, R.D.K. Misra, On Various Aspects of Decomposition of Austenite in a High-Silicon Steel During Quenching and Partitioning, Metall. Mater. Trans. A 45 (2014) 1247–1257. https://doi.org/10.1007/s11661-013-2053-8.

[23] S.J. Kim, H.S. Kim, B.C. De Cooman, Dilatometric Study of the Quench and Partitioning (Q& P) Process, Mater. Sci. (2007).

[24] E. De Moor, S. Lacroix, L. Samek, J. Penning, J.G. Speer, Dilatometric Study of the Quench and Partitioning Process Dilatometric Study of the Quench and Partitioning Process, (2014).

[25] P. Kantanen, M. Somani, A. Kaijalainen, O. Haiko, D. Porter, J. Kömi, Microstructural Characterization and Mechanical Properties of Direct Quenched and Partitioned High-Aluminum and High-Silicon Steels, Metals (Basel). 9 (2019). https://doi.org/10.3390/met9020256.

[26] S. Pashangeh, M. Somani, S.S. Ghasemi Banadkouki, Structure-Property Correlations of a Medium C Steel Following Quenching and Isothermal Holding above and below the M_s Temperature, ISIJ Int. 61 (2021) 442–451. https://doi.org/10.2355/isijinternational.ISIJINT-2020-355.

[27] A.K. Singh, D.K. Chouhan, B. Bhattacharya, S. Biswas, High strength-ductility combination by quenching and partitioning of a low carbon microalloyed dual-phase steel, Mater. Sci. Eng. A 870 (2023) 144854. https://doi.org/10.1016/j.msea.2023.144854.

[28] S. Yan, X. Liu, W.J. Liu, H. Lan, H. Wu, Microstructural evolution and mechanical properties of low-carbon steel treated by a two-step quenching and partitioning process, Mater. Sci. Eng. A 640 (2015) 137–146. https://doi.org/10.1016/j.msea.2015.05.058.

[29] E. Tkachev, S. Borisov, Y. Borisova, T. Kniaziuk, A. Belyakov, R. Kaibyshev, Austenite stabilization and precipitation of carbides during quenching and partitioning (Q&P) of low-alloyed Si–Mn steels with different carbon content, Mater. Sci. Eng. A 895 (2024) 146212. https://doi.org/https://doi.org/10.1016/j.msea.2024.146212.